Absorption in Packed Towers with Concurrent Downward High-Velocity Flows—II: Mass Transfer

Measurements were made of mass transfer coefficients with gas and liquid phase controlling resistance using a concurrent flow packed column with a wide range of operating conditions and four types of packing.

Mass transfer coefficients were much larger than those obtainable in countercurrent towers.

The results were correlated with dissipated energy values. The correlations obtained can be used to determine absorption efficiency. Experimental results show that the use of a high velocity concurrent flow column is particularly suitable when mass transfer is controlled by the liquid phase resistance with chemical reaction in the liquid.

A. GIANETTO
V. SPECCHIA
and
G. BALDI

Istituto di Chimica Industriale
Politecnico Torino, Italy

SCOPE

A number of problems concerning concurrent flow packed columns, such as pressure drop, hold-up, liquid distribution on the packing, and residence time distribution of the liquid and gas phases have been investigated. Yet little attention has been given to their internal mass transfer rate although this kind of apparatus is widely used in industrial processes, especially as chemical reactor (hydrocracking, heavy fuel hydrogenation, and hydrodesulphuration).

Following early work in this field by McIlvroid (1956) and Wen et al. (1963), Reiss (1967) determined the transfer coefficients k_L and k_G multiplied by the interfacial area a for ammonia absorption in water and oxygen desorption from water, using rings of various diameters as packing. His proposed correlations for k_La and k_Ga, while valid under his experimental conditions, made no reference to the hydrodynamic regimes set up within the column as a result of variations in phase flow rate.

Under concurrent flow conditions, there are four main hydrodynamic regimes: low gas and liquid velocities will result in a gas continuous flow (Larkins et al., 1961; Weekman and Myers, 1964; Prost, 1967) in which the behavior of the two phases is similar to that observed under countercurrent conditions when flow values are well below the loading point. An increase in either flow rate will be followed by an increasingly evident interaction between the two phases, seen first as ripples on the surface of the liquid (rippled flow), then as annular liquid droplet pistons (pulsing flow), and lastly as uniform entrainment of minute droplets by the gas (spray flow).

These droplets are formed by removal from the surface of the liquid licking the packing and by periodic expulsion of liquid in the packing channels.

The four regimes reflect changes in the hydrodynamic situation with different effects on interfacial areas and transfer coefficients.

In an earlier work (Gianetto et al., 1970) covering these regimes and 4 types of packing (6 mm glass spheres, 6 mm glass and ceramic rings, and 6 mm Berl saddles). a values were determined by gas absorption in the presence of variously fast chemical reactions in liquid phase with known kinetics. During pulsing flow and spray flow in particular, interfacial area was mainly due to droplet formation. a values in these regimes were then correlated as a function of the dissipated energy and geometrical characteristics of the packing. The purpose of this paper is to supplement the data relating to the operation of concurrent packed columns by determining mass transfer coefficients k_G and k_L and their dependence of the various operating parameters.

CONCLUSIONS AND SIGNIFICANCE

Although confined to employment in absorption and desorption operations requiring less than one theoretical equilibrium stage, concurrent packed columns offer a mass transfer efficiency that is considerably higher than that of conventional countercurrent columns. This is the result of their increased interfacial area, which may exceed the geometric area, and increased transfer coefficient values. Such enhancement is particularly apparent when transfer is controlled by resistance in the liquid phase where k_La increases are 40-fold for approximately 15-fold increase in

Correspondence concerning this paper should be addressed to A. Gianetto, Istituto di Chimica Industriale, Politecnico, C. so Duca degli Abruzzi, 24-10100, Torino, Italy.

velocity. Here, however, equilibrium limits are unfortunately more restrictive when physical absorption occurs. For this reason, concurrent columns may be of particular importance for gas absorption with chemical reaction. Such a high efficiency is, of course, obtained with gas and liquid superficial velocities, and hence pressure drops, that are much higher than those usually achieved in countercurrent packed columns.

The coefficient k_G increases slightly with increases in either the liquid or gas rate, while k_L is little affected by gas rate changes and increases considerably with the liquid rate. Mean k_L values about 10 times greater than those obtainable with countercurrent columns under normal conditions (Danckwerts and Sharma, 1966) were observed.

Correlations for k_G and k_L as a function of the dissipated energy valid for pulsing and spray flow and for all the types of packing employed were also found. In the case of k_G, the relation

$$\frac{k_G\epsilon}{v_G} = (0.0350 \pm 0.002)\left[\left(-\frac{\Delta P}{\Delta z}\right)\frac{g_c}{\overline{C}_{fu}(\rho_G v_G^2 + \rho_L v_L^2)}\right]^{0.98\pm0.07}$$

establishes a formal analogy between mass and momentum transfer within the system.

The equation for k_L is

$$\frac{k_L\epsilon}{v_L} = 0.0305\left\{\left[\left(-\frac{\Delta P}{\Delta z}\right)\frac{g_c\epsilon}{a_v \cdot \rho_L \cdot v_L^2}\right]^{0.066} - 1\right\}$$

The utility of the above correlations should be improved when the packing dimensions and the physical gas and liquid properties will be taken into consideration.

PREVIOUS WORK

In an earlier paper (Gianetto et al., 1970), interfacial areas a were determined in a concurrent packed column with various gas and liquid rates and four types of packings (6 mm glass spheres, 6 mm Berl saddles, 6 mm glass, and ceramic rings). Values were clearly dependent on the type of hydrodynamic regime. During gas continuous flow a values were nearly equal to those obtainable in countercurrent columns; increases in either gas and/or liquid rate led first to marked increases in a (rippled and pulsing flow), followed by minor increases (spray flow). In this case the interfacial area may be much larger than the geometrical packing area owing to droplet formation.

Physical properties of the phases being constant, droplet formation is obviously related to dissipated energy and will also be dependent on the free volume of the column in which the entrained droplets can move. A correlation was therefore proposed between interfacial areas, dissipated energy, and the geometrical characteristics of the packing. Statistical assessment of the results gave the following expression:

$$\frac{a}{a_v} = (0.81 \pm 0.02)\left[\left(-\frac{\Delta P}{\Delta z}\right)\frac{\epsilon}{a_v}\right]^{0.48\pm0.3} \qquad (1)$$

Under the experimental conditions, pulsing flow began when

$$\log\frac{v_G\rho_G + v_L\rho_L}{\epsilon} \geq 1 - \frac{1}{5}\log\frac{v_G\rho_G}{v_L\rho_L} \qquad (2)$$

These results, valid with the units shown in Notation, were used in the present research.

EXPERIMENT

Mass transfer coefficients were evaluated by means of a large series of experiments covering the absorption of NH_3 and desorption of O_2 with a controlling resistance in the gaseous and liquid phase respectively.

The apparatus consisted of a packed column fed with thermostated 20°C solution from a tank. The gas phase was supplied by a rotary pump. The flow diagram is shown in Figure 1.

The column was made of plexiglass and had an inside diameter of 80 mm. The top section (about 1 m long) consisted of a gas calming zone and was crossed by a bundle of stainless steel pipes. The liquid was passed through these pipes and then distributed over the packing.

The length of the section containing the packing could be varied as required since the column was composed of 100, 200, or 300 mm flange-jointed segments. Each segment had three suitably spaced pressure traps for determining pressure drop values and the total mean pressure within the segment itself.

The gas and liquid phases were separated at the bottom of the column below the packing support grid.

Samples for analysis were withdrawn continuously and independently for each phase both above and below the packing in as pure a state as possible.

In the NH_3 absorption experiments, gas was withdrawn below the packing by means of an upset truncated cone type cap welded below the grid and connected to the analyzer by a small pipe.

Liquid was also withdrawn below the packing via a pipe connected to the apex of an inverted conical device inserted in a hole in the support grid. The inside of the cone contained a special filling that allowed the liquid to percolate with a very small hold-up and prevented the infiltration of gas.

A stainless steel, slightly conical collector was used to withdraw liquid from below the packing in the O_2 desorption experiments (Figure 2). This was fitted with a ring of 6 small

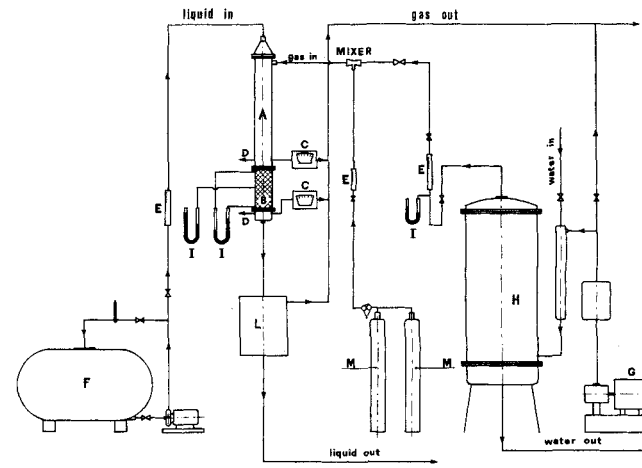

Fig. 1. Experimental apparatus: A, calming zone; B, packing zone; C, gas analyzers; D, liquid samples; E, rotameters; F, liquid tank; G, blower; H, air humidifier; I, manometers; L, liquid-gas separator; M, absorbable gas bottles.

exhaust funnels to carry off the gas with part of the liquid. The empty space below the support grid sharply reduced the velocity of the two phases. Part of the liquid was thus able to percolate into the center hole of the collector.

Both in NH_3 absorption and in O_2 desorption, particular care was always taken to avoid bubbling of gas into liquid samples and entrainment of liquid droplets in gas samples, especially by controlling the withdrawal rate. It was observed that condensation in the gas withdrawal tube had a remarkable effect on NH_3 concentrations in the bottom samples; this was avoided by heating the tube.

The packings used in interfacial area determinations were again employed. Their nominal diameter was 6 mm. Their geometrical properties are illustrated in Table 1.

A superficial velocity range of 0.25 to 4.3 and 38 to 222 cm/s was experimented for the liquid and gas phases respectively. As in the area measurement study, this range covered the several hydrodynamic regimes characteristic of a concurrent column.

MASS TRANSFER WITH CONTROLLING RESISTANCE IN GAS PHASE

Evaluation of the transfer coefficient in the gas phase was carried out by examining the absorption of an NH_3 and air mixture (7 to 7.5% by volume) in a liquid phase.

The absorbent liquid consisted of an aqueous solution 1M of sodium sulphate with virtually the same viscosity (1.54 ± 0.03 cp), density (1.08 ± 0.2 g/cm^3), and surface tension (40 ± 1 dynes/cm) values as the alkaline solutions used in the study of the transfer areas to obtain comparable a values.

NH_3 absorption occurs with a predominant resistance in the gas phase. This was checked numerically by assuming that the partial liquid phase mass transfer coefficient k_L was equal in practice to that determined in the O_2 desorption experiments (see later), under the same hydrodynamic conditions; this assumption was justified by the fact that $\mathcal{D}_{O_2} \simeq \mathcal{D}_{NH_3}$ in the liquid phase.

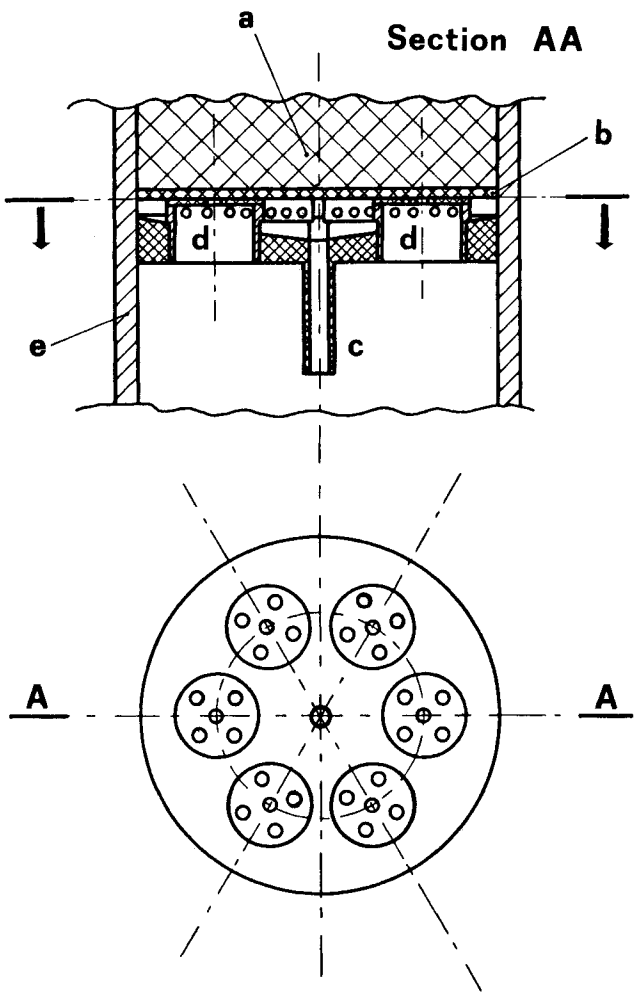

Fig. 2. Liquid sampling apparatus for O_2 desorption: a, packing; b, grid; c, liquid sample out; d, gas-liquid out; e, wall of the column.

The mean ratio between the partial and overall gas phase resistance was found to be over 90%.

An I.R. analyzer was used to analyze the gas phase at the packing inlet and outlet. NH_3 concentration in the liquid phase was determined by titration with a mixture of methyl red and methylene blue as indicator in accordance with the suggestion of Houston and Walker (1950); this mixture was not affected by the buffering action of the sodium sulphate in the solution.

The gas phase mass transfer coefficient K_Ga ($\simeq k_Ga$) was determined from the following design equation:

$$K_Ga \simeq k_Ga = \frac{G_mRT}{P_mZS[(1-y)_{ml}]_m} \int_{y_1}^{y_2} \frac{(1-y)_{ml}\,dy}{(1-y)(y^*-y)} \tag{3}$$

The integral was calculated numerically.

The NH_3 gas-liquid equilibrium conditions for a saline solution were determined from the following specially devised equation (Baldi and Specchia, 1971 a, b; see also Appendix).

$$y^* = \frac{c_{NH_3}}{P_m \cdot 10^{-hI}(A - B \cdot c_{NH_3})} \tag{4}$$

Piston flow was assumed for both phases when calculating k_Ga even though this is not exactly the case (Van Swaaij et al., 1969). Only very slight mass transfer coefficient variations, about that of the experimental error, would in fact result from taking axial dispersion into account. The same assumption was made for k_La calculations.

It was noted that k_Ga values varied by no more than 8% in response to a noticeable difference in NH_3 initial concentration in the gas phase (from 5.5 to 9.5%). Since withdrawals were made immediately below the grid, k_Ga values obtained by gas analysis may have been slightly too high, particularly at low liquid flow rates, due to gas-liquid transfer during passage through the grid. However, the discrepancy in the balance checks on the mass transferred between the two phases in each experiment was never more than 10%.

Figure 3 illustrates our k_Ga values correlations according to the procedure suggested by Reiss (1967) (results from about 180 experiments). The figure indicates the upper abscissa limit of the field explored by Reiss as well as his k_Ga interpolation line obtained with larger Raschig rings (up to 76 mm). Our data display greater scattering. This may be due to the fact that a greater range of liquid flows was explored; as can be seen, the sequences of points bearing the same symbol (at the same gas rate, for various liquid rates) show a behavior that differs from that of the general correlation line. It should be noted that Reiss's mean value was higher. On the other hand, when heating was used to eliminate condensation in the gas withdrawal pipe, the exit gas NH_3 concentration values were found to increase with a consequent decrease in k_Ga values. No reference to this problem is made by Reiss.

k_G values were then obtained from the k_Ga findings, using the area values obtained with correlation (1). Figure 4, for instance, illustrates k_G behavior patterns for Berl saddles versus v_G and v_L, gas and liquid phase superficial velocity (respectively). It will be seen that phase velocity

has little effect in increasing coefficient values; this is particularly true for not too low values of v_G. In this connection, it may be noted that Wen et al. (1963) obtained $k_G a$ values that decreased with v_L. They suggest that this was due to a decrease of a with v_L. This, however, is directly contrary to our findings.

The behavior patterns shown in Figure 4 can be interpreted in physical terms by reference to the fact that an increase in the real gas velocity in the packing, due to increases in v_G and/or v_L, may be responsible for an enlargement of the superficial area on account of droplet formation: the gas phase transfer coefficient, on the other hand, depends mainly on the relative velocity between the two phases and shows only a very slight increase.

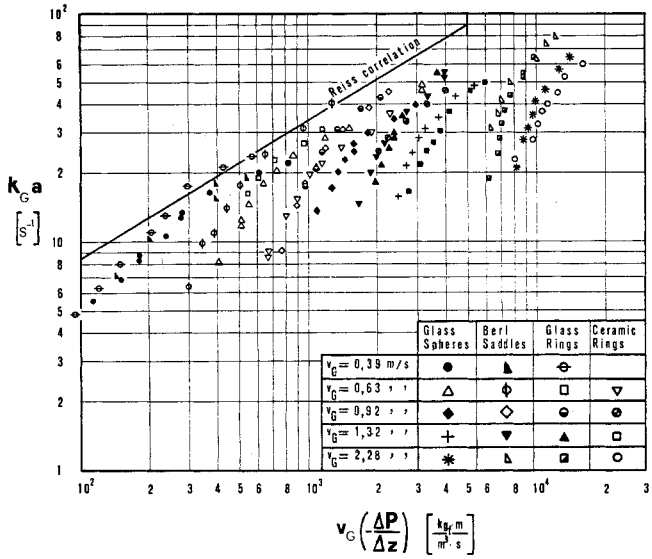

Fig. 3. Reiss's correlation for $k_G a$ values.

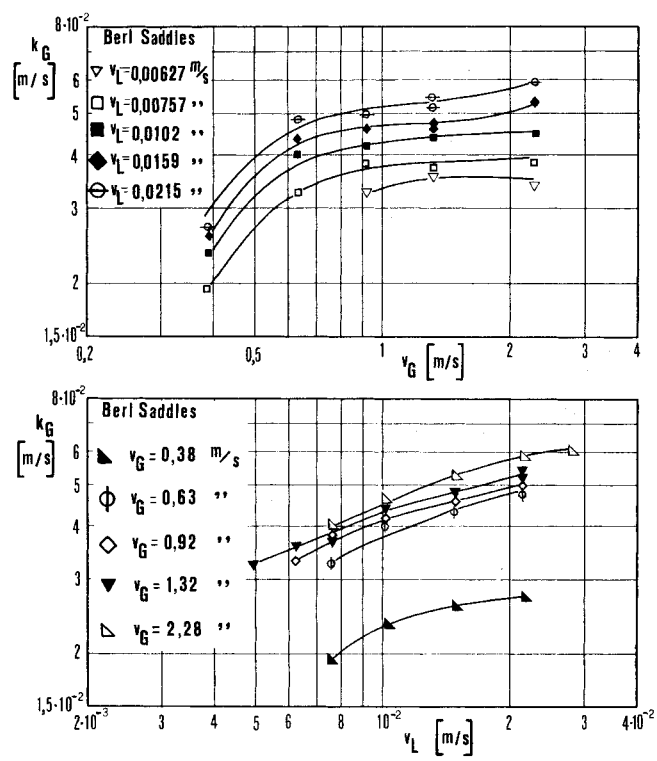

Fig. 4. k_G vs. gas phase superficial velocity v_G and liquid phase superficial velocity v_L for Berl saddles.

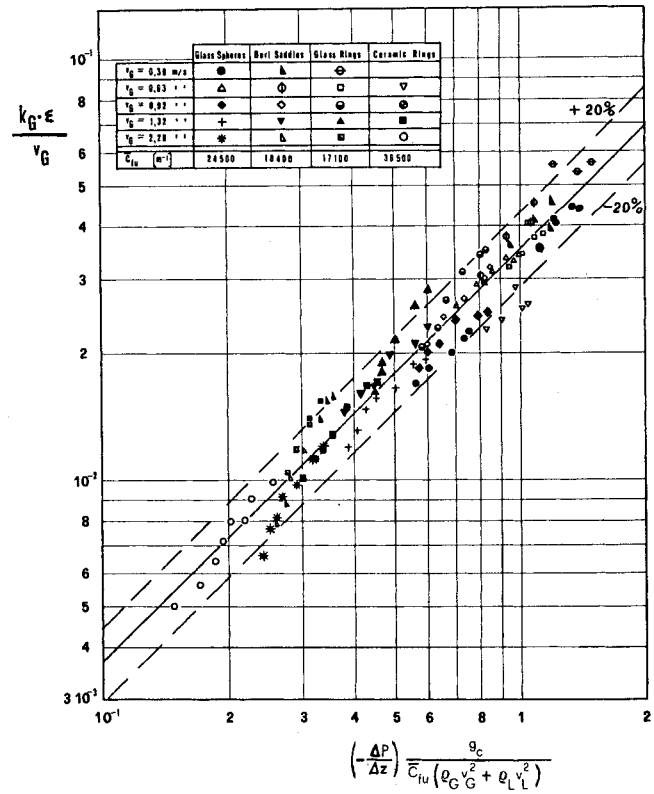

Fig. 5. Correlation for the gas phase mass transfer coefficient k_G.

TABLE 1. PACKING PROPERTIES

Type	Porosity ϵ	Geometrical area a_v $[m^{-1}]$	$\overline{C}_{fu}$ used in correlation (4) $[m^{-1}]$
Glass spheres 6 mm	0.41	590	24.500
Berl saddles 6 mm	0.59	900	18.400
Ceramic rings 6 mm	0.52	872	36.500
Glass rings 6 mm	0.70	891	17.100

In Figure 5, the ratio between mass transfer coefficient (in pulsing and spray flow only) and gas velocity in the empty spaces in the packing—this could be called the Stanton mass number—is expressed in function of a friction factor. This is modified by the presence of the two-phase flow and on account of form drag, expressed by a packing shape coefficient $\overline{C}_{fu}$ (Treybal, 1968), experimentally determined from pressure drop measurements with a wet packing, at v_L values tending to zero. Mean values of $\overline{C}_{fu}$ for the explored v_G range are given in Table 1. As can be seen in Figure 5 the experimental points fall within ± 20% of the interpolation value.

k_G values for gas continuous and rippled flow show a poor fit with this correlation, since power correlations are mainly significant when droplets formation occurs.

The interpolation line shows a relative mean quadratic error of 13.2%. Its analytical formula, with a statistical assessment of the data to a 99% degree of confidence, is as follows:

$$\frac{k_G \epsilon}{v_G} = (0.0350 \pm 0.002) \left[\left(-\frac{\Delta P}{\Delta z} \right) \frac{g_c}{\overline{C}_{fu}(\rho_G v_G^2 + \rho_L v_L^2)} \right]^{0.98 \pm 0.07} \quad (5)$$

In spite of the presence of form drag, the linearity is such as to suggest at least a formal analogy between mass and momentum transfer in the system. A similar proposal for solid-fluid mass transfer has already been made by Ergun (1952) for single-phase flows in granular beds*.

MASS TRANSFER WITH CONTROLLING RESISTANCE IN LIQUID PHASE

Mass transfer coefficients in liquid phase were measured on the assumption of absorption and desorption equivalence, that is, that the direction of transfer was irrelevant; this is particularly true when the concentration of the transferred component is too low to have any appreciable effect on the physical properties of the interface. These coefficients were studied by means of oxygen desorption with air from a 2N NaOH solution (as used in measuring interfacial areas) saturated with O_2 to a p_{O_2} value of about 500 to 550 mm/Hg.

Since O_2 was obviously poorly soluble in the liquid, the resistance to transfer was virtually confined to this phase. Since $\mathcal{D}_{O_2} \simeq \mathcal{D}_{NH_3}$ in the gas phase, the partial coefficient in this phase for O_2 desorption could be taken as practically equivalent to that for NH_3 absorption under the same hydrodynamic conditions. Thus the mean ratio between K_L and k_L was found to be over 0.99.

About 210 experiments were carried out. Polarographic analysis was done on the liquid phase only at both the inlet and outlet of the packing with a continuous analyzer. The calibration of the instrument was checked systematically. Particular care was taken to prevent pressure and temperature fluctuations in the measuring cells.

No useful analysis could be made of the gas phase, since there was no more than an extremely small variation in its O_2 content.

$k_La(\simeq K_La)$ was calculated by means of the following differential equation (piston flow for the two phases was still assumed):

$$-L\frac{dc_{O_2}}{dz} = k_La\,S(c_{O_2} - c^*_{O_2}) \qquad (6)$$

This was integrated numerically and k_La was determined by trial and error until the final concentration in the liquid, as calculated for $z = Z$, was equal to the experimentally observed value. Henry's gas-liquid equilibrium law was assumed to be valid and note was also taken of a linear variation in total pressure along the column since this had an appreciable effect on the value of the driving force.

Since the resistance to transfer was confined to the liquid phase on account of the very low O_2 concentrations, the effect of the stationary component could also be ignored. It was also shown that k_La values vary by no more than 7% in response to noticeable differences in packing height and initial driving force.

Figure 6, for instance, shows k_La and k_L values (the latter in the pulsing and spray flow range only) versus v_L using Berl saddles as packing.

It will be noted that k_La increases were 40-fold for approximately 15-fold increases in velocity. In the case of k_L, these increments were obviously less, although their magnitude nevertheless shows the notable efficiency of concurrent contact when the controlling resistance is in the liquid phase. Our results, together with those of

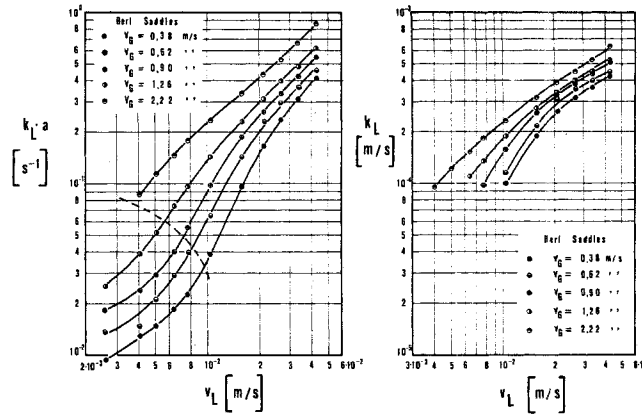

Fig. 6. k_La and k_L vs. liquid phase superficial velocity v_L for Berl saddles.

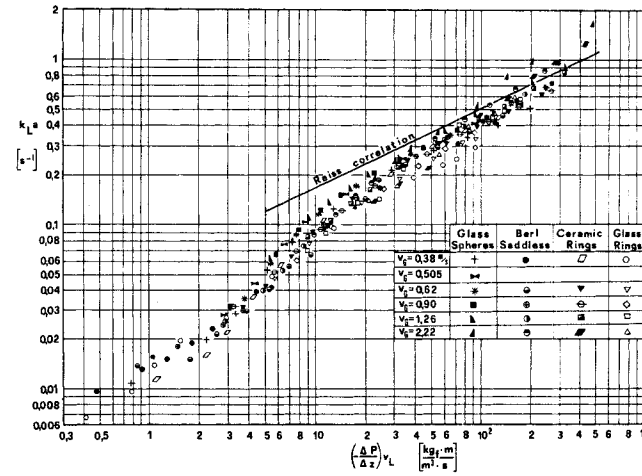

Fig. 7. Reiss's correlation for k_La values.

Danckwerts and Sharma (1966), indicate that concurrent column k_L values are on the average about 10 times greater than those obtained in countercurrent columns under normal working conditions.

Figure 7 shows our results of k_La correlated as they were proposed by Reiss (1967). The diagram contains also the interpolation line of the data obtained by Reiss; the limits of the field investigated by Reiss are also shown. On this occasion, too, our k_La were slightly lower than his, especially in the case of smaller abscissa values.

By analogy with Figure 5, the ratio $\dfrac{k_L\epsilon}{v_L}$ was also expressed in function of $\left(-\dfrac{\Delta P}{\Delta z}\right)\dfrac{g_c\epsilon}{a_v\,\rho_L\,v_L{}^2}$ in Figure 8 for pulsing and spray flow regimes; k_L values for gas continuous and rippled flow did not agree with this correlation.

This correlation illustrates the dependence of k_L on the hydrodynamic conditions of the liquid phase.

When the liquid percolates in the form of a film with a real velocity $u_L = \dfrac{v_L}{h_{L\epsilon}}$ where $\epsilon \cdot h_L$ is the liquid hold-up, the dependence of k_L on u_L can be postulated in the form

$$k_L \propto \sqrt{u_L} \quad \text{or} \quad k_L \propto u_L{}^{3/2}$$

on the base of Levich's theoretical proposal (1962) for mass transfer in a laminar and turbulent falling film respectively.

* Pressure drop correlations for concurrent flow in packed columns are reported in the literature (Larkins et al., 1961; Weekman and Myers, 1964; Charpentier et al., 1969).

When droplets are involved, on the other hand, unsteady transfer theory postulates inverse proportionality between k_L and the square root of the exposure time, that is, the period between the moment of droplet formation and that of its impact and remixing on the packing walls. Since this time is, in practice, in inverse proportion to u_L for a given packing size, it follows that $k_L \propto \sqrt{u_L}$.

Assuming, therefore, as an approximation:

$$k_L \propto u_L$$

the definition of u_L gives

$$\frac{k_L \epsilon}{v_L} \propto \frac{1}{h_L}$$

h_L was correlated by Larkins et al. (1961), Reiss (1967), and Bakos and Charpentier (1970) in function of the ratio between the single-phase flow pressure drop of the liquid and of the gas. Alternatively, this ratio has been also expressed in function of that between the total pressure drop $\left(-\frac{\Delta P}{\Delta z}\right)$ and the liquid phase pressure drop alone; the latter is proportional to $\frac{\rho_L v_L^2}{d}$ where d is the packing hydraulic diameter, so that $d \propto \frac{\epsilon}{a_v}$.

It therefore follows that $\frac{1}{h_L}$ is a function of $\frac{\left(-\frac{\Delta P}{\Delta z}\right)\epsilon}{\rho_L v_L^2 a_v}$ as was stated in Figure 8.

A slightly greater range of scatter was found than in the k_G correlation, particularly for low liquid velocities.

The following expression gives the most simple interpolation formula for the experimental data, with a relative mean quadratic error of 14.3%:

$$\frac{k_L \epsilon}{v_L} = 0.0305 \left\{ \left[\left(-\frac{\Delta P}{\Delta z} \right) \frac{g_c \epsilon}{a_v \rho_L v_L^2} \right]^{0.068} - 1 \right\} \quad (7)$$

It can be seen that $\frac{k_L \epsilon}{v_L}$ is only slightly dependent on the ratio between the total dissipated energy $\left(-\frac{\Delta P}{\Delta z}\right)$ and the energy of the liquid; hence k_L must be considered almost proportional to v_L.

Illustration of the dependence of k_L on u_L is given in Figure 9, where, for calculations of u_L, h_L values have been reckoned according to Larkins et al. (1961). To cover all the types of packing adopted, $k_L a_v$ is inserted on the ordinate. Here a_v (geometric area per unit volume) takes account of the influence of packing shape on film thickness for a given u_L value.

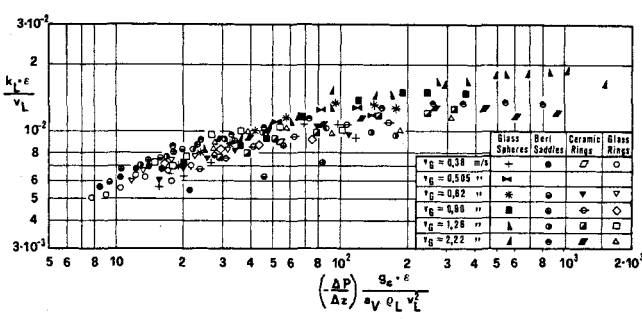

Fig. 8. Correlation for the liquid phase mass transfer coefficient k_L.

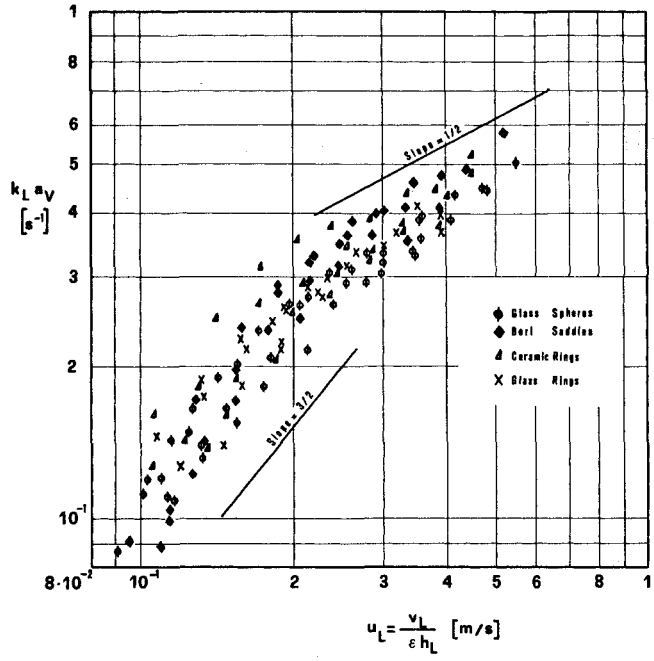

Fig. 9. $k_L a_v$ vs. the mean real liquid phase velocity u_L.

If the approximation required for the calculation of h_L is ignored, it will be found $k_L \propto u_L^n$: for lower u_L values, when there is probably a prevalently turbulent film flow, it is $n \simeq 3/2$, as reported by Levich (1962); for higher u_L values in the presence of droplet flow, it is $n \simeq 1/2$.

ACKNOWLEDGMENT

This work was carried out with the financial support of C.N.R.

NOTATION

A = temperature dependent coefficient for NH_3 solubility, kmoles/m^3 atm
a = interfacial area per unit volume of column, m^{-1}
a_v = geometrical area per unit volume of column, m^{-1}
B = temperature dependent coefficient for NH_3 solubility, atm^{-1}
$\overline{C_{fu}}$ = packing shape coefficient for a wet packing, m^{-1}
c_{H_2O} = H_2O concentration in liquid phase, kmoles/m^3
$\overline{c_{H_2O}}$ = H_2O mean concentration in liquid phase, kmoles/m^3
c_{NH_3} = NH_3 concentration in liquid phase, kmoles/m^3
c_{O_2} = O_2 concentration in liquid phase, kmoles/m^3
$c^*_{O_2}$ = O_2 concentration in liquid phase in equilibrium with gas phase, kmoles/m^3
d = packing hydraulic diameter, m
g_c = conversion factor, kg$_m$ · m/kg$_f$ · s^2
G_m = mean molar gas rate, kmoles/s
H, H_∞ = coefficients of the formula (A2), atm^{-1} · (kmoles/m^3)$^{1-\alpha}$
H^* = coefficient of the formula (A3), atm^{-1}
h = coefficient dependent on temperature and ions species in liquid phase, m^3/kion
h_L = fraction of void occupied by liquid phase, dimensionless
K_G, k_G = overall and partial gas phase mass transfer coefficients m/s
k_i = parameter defined by formula (A4), m^3/kion
K_L, k_L = overall and partial liquid phase mass transfer coefficients, m/s
k_y = gas phase mass transfer coefficient, kmoles/m^2 · s

I = ionic strength in liquid phase, kions/m^3
L = liquid flow rate, m^3/s
n = coefficient of dependency between k_L and u_L, dimensionless
P_m = mean pressure in column, atm
$\left(-\frac{\Delta P}{\Delta z}\right)$ = pressure drop, kg$_f$/m^3
Q = heat developed from solubilization of 1 kmole of NH_3, kcal/kmole
R = gas constant, m^3 atm/kmole °K
S = section of the column, m^2
T = absolute temperature, °K
u_L = real liquid phase velocity, m/s
v_G = superficial velocity of gas phase, m/s
v_L = superficial velocity of liquid phase m/s
Z = packing height, m
z = distance from the top of the packing, m
y = molar fraction of NH_3 in gas phase, dimensionless
y^* = molar fraction on NH_3 in gas phase in equilibrium with c_{NH_3}, dimensionless

Greek Letters

α = number of H_2O molecules bound to 1 molecule of NH_3, dimensionless
γ_i = activity coefficient, dimensionless
ϵ = packing porosity, dimensionless
ρ_G = gas phase density, kg/m^3
ρ_L = liquid phase density, kg/m^3

LITERATURE CITED

Bakos, M., and J. C. Charpentier, "Taux de rétention pour des écoulements gaz-liquide à co-courant vers le bas dans les colonnes à garnissage arrosé et noyé," *Chem. Eng. Sci.*, **25**, 1822 (1970).

Baldi, G., and V. Specchia, "Solubilità dell'ammoniaca in acqua," *La Chim. l'Ind.*, **53**, 929 (1971a).

———., "Solubilità dell'ammoniaca in soluzioni saline," *ibid.*, 1022 (1971b).

Charpentier, J. C., C. Prost, and P. Le Goff, "Chute de pression pour des écoulements à co-courant dans les colonnes à garnissage arrosé: comparaison avec le garnissage noyé," *Chem. Eng. Sci.*, **24**, 1777 (1969).

Danckwerts, P. V., and M. M. Sharma, "The Absorption of Carbon Dioxide into Solutions of Alkalis and Amines," *Chem. Eng.*, **202**, 244 (1966).

Ergun, S., "Mass Transfer Rate in Packed Columns—Its analogy to Pressure Loss," *Chem. Eng. Progr.*, **48**, 227 (1952).

Gianetto, A., G. Baldi, and V. Specchia, "Absorption in Packed Towers with Cocurrent Downward High-Velocity Flows, I: Interfacial Areas," *Quad. Ing. Chim. Ital.*, **6**, 125 (1970).

Houston, R. W., and C. A. Walker, "Absorption in Packed Towers—Effect of Molecular Diffusivity on Gas Film Coefficient," *Ind. Eng. Chem., Int. Edit.*, **42**, 1105 (1950).

Larkins, R. B., R. R. White, and D. W. Jeffrey, "Two-Phase Cocurrent Flow in Packed Beds," *AIChE J.*, **7**, 231 (1961).

Levich, V. G., *Physicochemical Hydrodynamics*, 2nd. edit., pp. 694, Prentice-Hall, Englewood Cliffs, N. J. (1962).

Onda, K., E. Sada, T. Tobayashi, S. Kito, and K. Ito, "Salting-out Parameters of Gas Solubility in Aqueous Salt Solution," *J. Chem. Eng. Japan*, **3**, 18 (1970).

Prost, C., "Etude des fluctuations de la texture du liquide s'écoulant à contre-courant ou à co-courant du gaz dans un garnissage de colonne d'absorption," *Chem. Eng. Sci.*, **22**, 1283 (1967).

Reiss, L. P., "Cocurrent Gas-Liquid Contacting in Packed Columns," *Ind. Chem. Eng., Process Design Develop.*, **6**, 486 (1967).

Treybal, R. F., *Mass Transfer Operations*, 2nd. edit., p 161, McGraw-Hill, New York (1968).

Van Krevelen, D. W., and P. J. Hoftijzer, "Sur la Solubilité des Gas dans les Solutions aqueuses," *Chim. Ind., XXIeme Cong. Int. Chim. Ind.*, 168 (1950).

Van Swaaij, W. P. M., J. C. Charpentier, and J. Villermaux, "Residence Time Distribution in Liquid Phase of Trickle Flow in Packed Columns," *Chem. Eng. Sci.*, **24**, 1083 (1969).

Weekman, V. W., and J. E. Myers, "Fluid—Flow Characteristics of Cocurrent Gas-Liquid Flow in Packed Beds, *AIChE J.*, **10**, 951 (1964).

Wen, C. Y., W. S. O. Brien, and L. T. Fan, "Mass Transfer in Packed Beds Operated Cocurrently," *J. Chem. Eng. Data*, **8**, 42 (1963).

APPENDIX

Solubility of Ammonia in Water and Saline Solutions

The absorption of ammonia in water may be assumed to give rise to hydrates whose general formula is $NH_3 \cdot \alpha H_2O$. These are derived from reactions between the physically dissolved NH_3 (proportional to y^*P) and the H_2O still available ($c_{H_2O} - \alpha c_{NH_3}$). Ammonia solubility can be expressed in the form:

$$c_{NH_3} = H\, y^*\, P\, (c_{H_2O} - \alpha c_{NH_3})^\alpha \qquad (A1)$$

This expression gives a good fit (mean error: about 2%) with the experimental data for c_{NH_3}/c_{H_2O} ratios up to about 0.4.

α was equal to 1.11, irrespective of concentration and temperature; H, on the other hand, displayed an exponential dependence on temperature:

$$H = H_\infty\, e^{Q/RT} \qquad (A2)$$

where Q = heat developed from the solubilization of 1 kmole of NH_3 (8100 kcal/kmole).

Since $\alpha \simeq 1$, the solubility expression can be simplified to

$$\frac{c_{NH_3}}{c_{H_2O}} \simeq \frac{H\, c_{H_2O}^{\alpha-1}\, y^*\, P}{1 + \alpha^2\, H\, c_{H_2O}^{\alpha-1}\, y^*\, P} \simeq \frac{H^*\, y^*\, P}{1 + \alpha^2\, H^*\, y^*\, P} \qquad (A3)$$

where H^* is practically constant with respect to concentration and varies with temperature in the same way as H.

When electrolytes are dissolved in the water, the presence of ions changes the activity coefficients (γ_i) of the molecular species. This variation has been stated in the following form by several authors (Van Krevelen and Hoftijzer, 1950; Onda et al., 1970):

$$\gamma_i = 10^{k_i I} \qquad (A4)$$

where I is the ionic strength of the electrolyte and k_i is a parameter that is independent of I, but dependent on electrolyte type and on temperature. Inclusion of this equation gives the expression:

$$\left(\frac{c_{NH_3}}{c_{H_2O}}\right)_{\text{sal.sol.}} = \frac{H^*\, 10^{-hI}\, y^*\, P}{1 + \alpha^2\, H^*\, 10^{-hI}\, y^*\, P} \qquad (A5)$$

The salting-out parameter h is a function of temperature and ion species; as a first approximation, it may be calculated by the addition of different factors, depending on the cations, anions, and dissolved gas (Onda et al., 1970). Experimentation of gas solubility in a given saline solution will therefore be necessary if exact values are required. Both these procedures were followed in the present work to check the value of h.

Since c_{H_2O} did not vary more than 3% for the NH_3 absorption in the column, it was assumed as a constant and equation (A5) was expressed in the form:

$$y^* \simeq \frac{c_{NH_3}}{P_m \cdot 10^{-hI}\, (H^*\, \bar{c}_{H_2O} - H^*\, \alpha^2\, c_{NH_3})} = \frac{c_{NH_3}}{P_m \cdot 10^{-hI}\, (A - B\, c_{NH_3})} \qquad (A6)$$

where y^* is the molar fraction of the NH_3 in gas phase in equilibrium with c_{NH_3}, P_m is the mean pressure in the column and $\bar{c}_{NH_3}$ is the mean molar concentration of H_2O in liquid phase.

Manuscript received October 12, 1972; revision received March 15 and accepted April 9, 1973.